



Growth and LC-PUFA production of the cold-adapted microalga *Koliella antarctica* in photobioreactors

Hirono Suzuki¹ · Chris J. Hulatt^{1,2}  · René H. Wijffels^{1,3} · Viswanath Kiron¹

Received: 30 April 2018 / Revised and accepted: 13 August 2018
© The Author(s) 2018, corrected publication 2018

Abstract

Microalgae are excellent sources of polyunsaturated fatty acids (PUFAs), but only a few species have been thoroughly investigated in controlled photobioreactor conditions. In this work, the cold-adapted microalga *Koliella antarctica* (Trebouxiophyceae) was cultivated at 15 °C to optimize growth and PUFA production in bubble-tube and flat-plate photobioreactors. The impact of nitrogen starvation, phosphorus starvation, salinity, and light intensity on the growth, fatty acid, and protein content was investigated. After culture optimization, a maximum biomass productivity of 2.37 g L⁻¹ day⁻¹ and maximum cell density of 11.68 g L⁻¹ were achieved. Among all conditions tested, the maximum total fatty acid (TFA) content measured 271.9 mg g⁻¹ dry weight in the late stationary phase. Nitrogen and phosphorus starvation strongly induced neutral lipid (TAG) accumulation, up to 90.3% of TFA, which mostly consisted of the monounsaturated fatty acid C18:1n-9 (oleic acid, OA). PUFAs were also abundant and together accounted for 30.3–45.8% of total triacylglycerol (TAG). The highest eicosapentaenoic acid (EPA) content (C20:5n-3) amounted to 6.7 mg g⁻¹ dry weight (4.9% TFA) in control treatments, while the highest arachidonic acid (ARA) content (C20:4n-6) was 9.6 mg g⁻¹ dry weight (3.5% TFA) in the late stationary phase. Phosphorus starvation was an effective strategy to obtain high total fatty acid yields (mg L⁻¹) while maintaining the protein, total PUFA, and omega-3 fatty acid contents.

Keywords Omega-3 fatty acid · LC-PUFA · Eicosapentaenoic acid (EPA) · Flat-plate photobioreactor · Triacylglycerol · Cold-adapted microalgae

Introduction

Microalgae are excellent sources of bioactive compounds that are known to benefit animal and human health (Borowitzka 2013). Among them are polyunsaturated fatty acids (PUFAs), particularly long-chain PUFAs (LC-PUFAs) with carbon

chain lengths of C20 and above. Especially, eicosapentaenoic acid (EPA, C20:5n-3), docosahexaenoic acid (DHA, C22:6n-3), and arachidonic acid (ARA, C20:4n-6) are important dietary components for animals and humans (Khozin-Goldberg et al. 2011; Martins et al. 2013). At present, LC-PUFAs are mostly derived from fish oils, but cultivated microalgae could provide natural and healthy vegetarian alternatives with lower environmental impacts (Wijffels and Barbosa 2010; Khozin-Goldberg et al. 2011; Chisti 2013). Although research on microalgae-derived PUFAs is very promising, only a few species have been thoroughly investigated in intensive cultivation systems. For example, the model microalgae *Phaeodactylum tricornerutum* and *Nannochloropsis* sp. have been studied for EPA production (Chrismadha and Borowitzka 1994; Mühlroth et al. 2013), while *Isochrysis galbana* has been cultivated for DHA production (Liu et al. 2013; Marchetti et al. 2018). However, these strains are mostly from temperate or warm water habitats and often perform best at temperatures around 25 °C. Bioprospecting and optimization of PUFA-rich strains that are able to grow rapidly at lower temperatures could enable year-round utilization of

Electronic supplementary material The online version of this article (<https://doi.org/10.1007/s10811-018-1606-z>) contains supplementary material, which is available to authorized users.

✉ Chris J. Hulatt
christopher.j.hulatt@nord.no; chulatt@mines.edu

¹ Faculty of Biosciences and Aquaculture, Nord University, Bodø, Norway

² Department of Chemistry, Colorado School of Mines, Golden, CO 80401, USA

³ Bioprocess Engineering, AlgaePARC, Wageningen University, Wageningen, The Netherlands

culture facilities in temperate zones and promote microalgae cultivation in cooler climates (Kvíděrová et al. 2017).

Cold-adapted microalgae from polar habitats recently gained attention not only for PUFA production (Teoh et al. 2004; Spijkerman et al. 2012; Artamonova et al. 2017) but also for their potential to achieve relatively high productivity at lower water temperatures (Hulatt et al. 2017). Their evolutionary adaptations have enabled them to successfully colonize many low-temperature areas, including glaciers, sea ice, and polar and alpine regions, which are often characterized by large seasonal fluctuations in environmental factors such as light and osmotic stress (Morgan-Kiss et al. 2006; Procházková et al. 2018). Such adaptations could benefit industrial cultivation systems, where microalgae often encounter fluctuations in light intensity, low temperature, and variable salinity, each of which can impact productivity. Of special interest is the elevation of PUFA levels in the membrane lipids of cold-adapted microalgae, which is one of the key adaptive strategies used to increase membrane fluidity and thereby maintain cell metabolism at lower water temperatures (Morgan-Kiss et al. 2006; Boelen et al. 2013). Cold-adapted microalgae might therefore be more productive sources of PFAs and other algae derivatives that could be used in food or feed products.

In microalgae cell cultures, abiotic factors, such as temperature, salinity, light, and nutrient availability, can be altered to induce high-value fatty acid production. Although physiological responses to these stressors are often species- or strain-specific, the accumulation of fatty acids is often coincident with reduced growth rates, leading to a net reduction in fatty acid productivity (Chen et al. 2017). Moreover, the main storage lipids in microalgae are triacylglycerols (TAG) that accumulate under stress conditions and are often comprised by saturated and mono-unsaturated fatty acids (Sharma et al. 2012). This in turn alters microalgae oil quality and its nutritional profile, e.g., reducing the proportion of PFAs. The best culture conditions should therefore be carefully selected to maximize the production of PFAs (Markou and Nerantzis 2013).

The cold-adapted microalga *Koliella antarctica* (Trebouxiophyceae, Andreoli et al. 1998) is a potential candidate for PUFA production and is reported to synthesize LC-PFAs (Lang et al. 2011). *Koliella antarctica* was originally isolated from ice-free seawater collected at a depth of 3 m in Terra Nova Bay, Ross Sea, Antarctica, at $-1.5\text{ }^{\circ}\text{C}$ (Andreoli et al. 1998). This species can grow at low temperatures down to $2\text{ }^{\circ}\text{C}$ and achieves maximum growth at $15\text{ }^{\circ}\text{C}$ (Vona et al. 2004). However, the best cultivation conditions for *K. antarctica* to obtain optimal growth and lipid production are not reported. In particular, detailed information on its fatty acid profile, LC-PUFA content, and TAG composition is not available.

The aim of this work was to optimize the growth and fatty acid production of *K. antarctica* in controlled photobioreactors, as a potential PUFA-rich feedstock for food and feed products. The impacts of nitrogen starvation, phosphorus starvation, salinity, and light intensity on the growth, fatty acid composition, and protein content of *K. antarctica* were investigated. Polar lipids and TAG were separated, and changes in the fatty acid profiles of these fractions were characterized. The effect of light intensity on the growth rate and photosynthetic efficiency of *K. antarctica* was subsequently measured using flat-plate photobioreactors.

Materials and methods

General cultivation conditions

Koliella antarctica strain SAG 2030 (Chlorophyta, Trebouxiophyceae) was obtained from the Culture Collection of Algae at Göttingen University (SAG, Germany). Stock cultures were retained on 1.2% agar plates as unialgal colonies and, prior to the experiments, were grown in 250 mL Erlenmeyer flasks containing Bolds Basal Medium (BBM) (Bischoff and Bold 1963). The Erlenmeyer flasks were supplied with a photosynthetic photon flux density (PPFD) of $90 \pm 20\text{ }\mu\text{mol photons m}^{-2}\text{ s}^{-1}$ using cool white fluorescent lamps. A temperature of $15\text{ }^{\circ}\text{C}$ was maintained throughout all the experiments, which is representative of summer conditions in cool climates and winter temperatures in warmer parts of the world. The bioreactor vessels and nutrient media used in each set of the following experiments were sterilized by autoclave ($121\text{ }^{\circ}\text{C}$, 20 min).

Salinity experiment in 100 mL bubble tubes

Koliella antarctica was cultivated in 27-mm-diameter glass bubble tubes containing 80 mL of BBM (Table 1, Fig. 1) to which different amounts of artificial sea salt were added. Salinities 0, 2, 4, 8, 16, and 32‰ were tested, and cultures were illuminated at $80\text{ }\mu\text{mol photons m}^{-2}\text{ s}^{-1}$ using cool white fluorescent lamps. Each treatment was maintained in a climate-controlled incubator (Termaks AS, Bergen, Norway), and the tubes with different treatments were randomized. Air containing 1.0% CO_2 was supplied to each of the cultures at a flow rate of 100 mL min^{-1} . Addition of CO_2 was controlled by a precision gas mixer (Photon Systems Instruments, Czech Republic) and delivered to each tube by individual rotameters (FL-2000, Omega, UK). To mitigate evaporation, the gas stream was bubbled through a humidifier, an autoclaved 1.0 L glass bottle containing Milli-Q water. Samples for biomass measurement were taken daily over a two-week cultivation period, and each treatment was performed in duplicate.

Table 1 Summary of experimental treatments in this study

Experiment	Reactor type	Volume (mL)	Light intensity ($\mu\text{mol photons m}^{-2} \text{s}^{-1}$)	Treatment	Salinity (‰)	Nutrient medium	CO ₂ (%)
Salinity	Bubble tubes	100	80	–	0, 2, 4, 8, 16, 32	BBM	1
Stress	Bubble tubes	350	120	Control	4	3N-BBM	1
Stress	Bubble tubes	350	120	N starvation	4	3N-BBM without nitrate	1
Stress	Bubble tubes	350	120	P starvation	4	3N-BBM without phosphate	1
Stress	Bubble tubes	350	120	HS	32	3N-BBM	1
Li-Ex I	Flat plate	380	70, 250, 500	–	4	2N-BBM	1
Li-Ex II	Flat plate	380	500	–	4	3× 3N-BBM	5

BBM is Bold's basal medium in its original formulation, while 3N-BBM is the common adjustment where the nitrate concentration is increased three-fold (3N). Additional adjustments were made for individual experiments, where 2N-BBM corresponds to double the concentration of nitrate, and 3× 3N-BBM is 3N-BBM formulation at three-fold its original concentration. The soil extract component of Bold's basal medium remained the same in all of the media in this study.

Stress experiment in 350 mL bubble tubes

In this experiment, larger 350 mL glass bubble tubes (Fig. 1) were used to test the effect of nitrogen (N⁻), phosphorus (P⁻), and high salinity (HS) stress conditions on growth, fatty acid, and protein production. These larger tubes were also supplied with air containing 1.0% CO₂ at a flow rate of 100 mL min⁻¹, but the PPFD was increased to 120 $\mu\text{mol photons m}^{-2} \text{s}^{-1}$. Cultures used in all experimental treatments were initially grown in the same complete 3N-BBM medium (BBM with 3-fold nitrate; see Table 1). When the cultures reached the exponential phase, the cells were centrifuged (3500 ×g, 5 min), washed, and resuspended in one of four experimental media. The four treatments were (a) control (3N-BBM); (b) nitrate free, N⁻ (3N-BBM without NaNO₃); (c) phosphate free, P⁻ (3N-BBM without KH₂PO₄ or K₂HPO₄); and (d) high salt, HS (3N-BBM with artificial sea salt added to 32 g L⁻¹) (Table 1). After washing and resuspending in the experimental media, the starting cell density of each tube was approximately the same at 0.3 g L⁻¹ dry weight. The time of washing and the application of experimental treatments was designated at the start of the experiment ($t = 0$), and the subsequent cultivation time was 5 days. Each treatment was performed in triplicate and randomly assigned to one of the bioreactors.

Light experiments in flat-plate photobioreactors

Koliella antarctica was cultivated in 380 mL flat-plate photobioreactors (Algaemist-S, Wageningen UR, The Netherlands) for 18 days, as shown in Fig. 1. The reactor cultivation vessel, which had a 14 mm light path, was illuminated continuously with warm white LEDs from one side. Cultures were sparged with 0.2 μm filtered air (Acrodisc PTFE filters, Pall Corporation, USA) enriched with either 1.0 or 5.0% CO₂ (Table 1). The cultivation temperature was accurately controlled with an external cooling system (Julabo F25, JULABO GmbH, Germany) and an internal heating system, maintaining 15 ± 0.4 °C. To mitigate evaporation, Milli-Q water was added with a syringe via the sample port. The PPFD impinging on the front of the cultivation vessel was measured with a Li-Cor189 2 π quantum sensor. The output PPFD (the light transmitted through the reactor) was determined by calibrating the photobioreactor-transmitted light sensor with the LiCor sensor. Both incident and transmitted light measurements were the average values obtained at 28 positions on each face. In the first experiment (Li-Ex I), the PPFD on the front surface was 23 $\mu\text{mol photons m}^{-2} \text{s}^{-1}$ for the first six days, to avoid immediate light stress, then increased to either 70, 250, or 500 $\mu\text{mol photons m}^{-2} \text{s}^{-1}$. In the second experiment (Li-Ex II) with higher nutrient concentrations, only 500 $\mu\text{mol photons m}^{-2} \text{s}^{-1}$ was supplied. For each of the cultures in Li-Ex I, the optical density of the

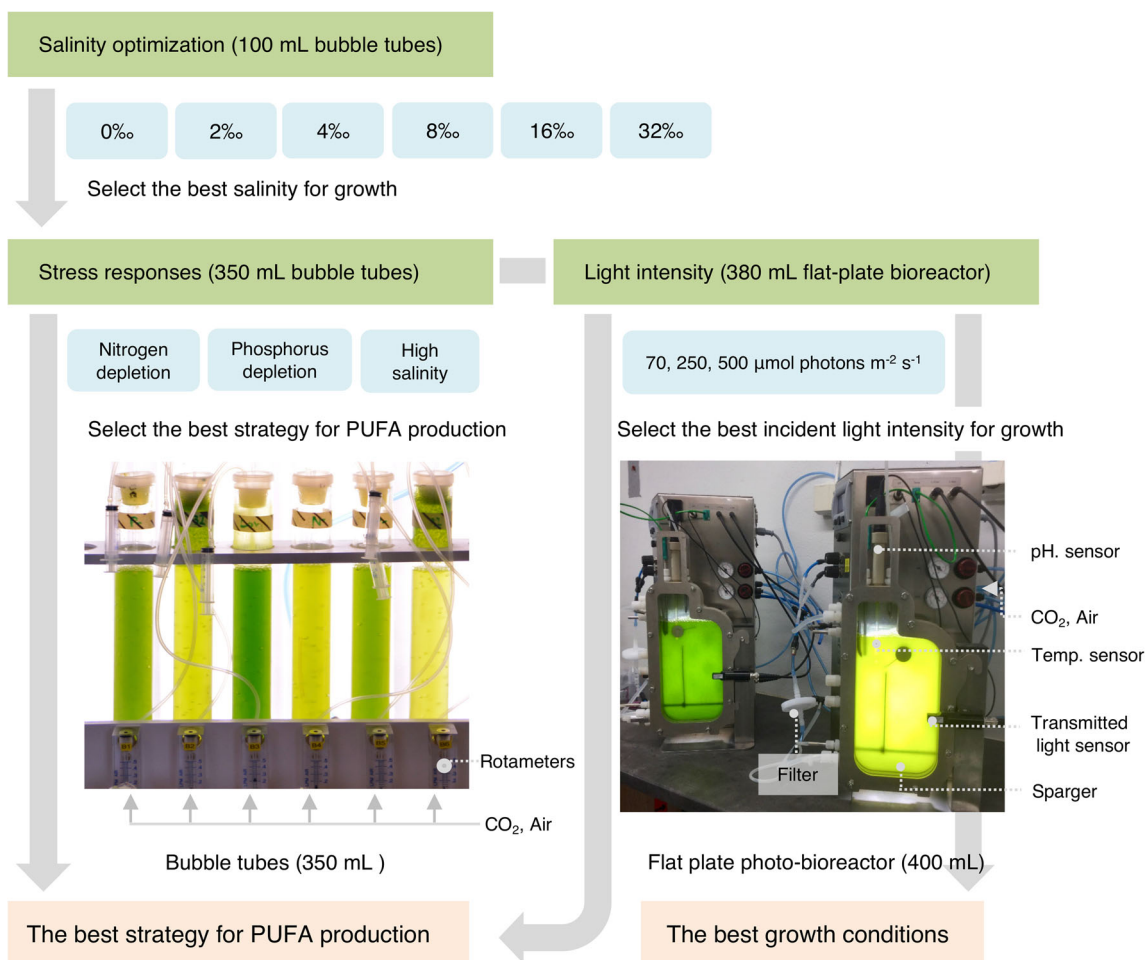


Fig. 1 Experimental design and two types of photobioreactor used in the present study including bubble-tube (left) and flat-plate photobioreactors with 14 mm light path length (right)

inoculum was measured and the volume adjusted to achieve the same starting cell density for each experimental replicate.

Growth measurements

The growth of *K. antarctica* was measured by the optical density, which was calibrated against the dry weight. The optical density was determined by measuring the absorbance at 540 and 680 nm in a 1 cm semi-micro cuvette. The samples were diluted with medium (1- to 50-fold) to maintain the absorbance reading below 1.0 for linear response. The dry weight of 26 samples from different experiments and time points were also determined by filtering 10 mL of culture broth through pre-weighed $\sim 1.0 \mu\text{m}$ pore size 47-mm glass fiber filters (VWR, Norway). Filters were then rinsed with isotonic ammonium formate (0.5 M for salinity and stress experiments, 0.06 M for the flat-plate photobioreactors) to remove extracellular salt and dried at 95°C for 48 h. Filters were subsequently re-weighed, and the dry weight (g L^{-1}) was calculated. The dry weight was related to the absorbance at 540 nm as shown in Eq. (1) ($R^2 = 0.99$, $n = 26$).

$$DW = (0.295 \cdot A_{540}) + 0.088 \quad (1)$$

where DW is the calculated dry weight (g L^{-1}) based on the absorbance at 540 nm (A_{540}). The absorbance ratio (A_{680}/A_{540}) was also determined to indicate the ratio of pigments (mainly chlorophyll) to the biomass. Samples for further biochemical analysis were obtained by pelleting cells in 2.0 mL microcentrifuge tubes, washing with isotonic ammonium formate to remove salt, then stored at -40°C .

Nutrients

Samples for nitrate and phosphate analysis were centrifuged ($3500 \times g$, 5 min), and the supernatant was stored at -40°C . The extracellular nitrate and phosphate concentrations were measured with standard colorimetric methods as described by Ringuelet et al. (2011). Nitrate was reduced to nitrite by NADH:nitrate reductase (NECi Superior Enzymes, Lake Linden, USA) and measured at 540 nm using a 96-well microplate. Extracellular phosphate was determined using the ascorbic acid/molybdate method, and the absorbance of the

colored complex was measured at 880 nm. Nitrate and phosphate uptake rates ($\text{mM L}^{-1} \text{ day}^{-1}$) were calculated by dividing the change in nutrient concentrations by the difference in time, and the maximum values are reported.

Fatty acid analysis of polar lipids and TAG

Total lipids were extracted from approximately 7 mg of freeze-dried biomass using 4.0 mL of chloroform:methanol (2:2.5 v/v) containing internal standard (tripentadecanoin, C15:0 triacylglycerol, Sigma-Aldrich, Norway). A bead mill (Precellys 24, Bertin Technologies, France) and 0.1 mm glass beads were used for cell lysis. Lipids were recovered by addition of 2.5 mL Tris buffer (6 g L^{-1} Tris, 58 g L^{-1} NaCl, pH 7.5) followed by vortexing (10 s) and centrifugation ($1500 \times g$, 5 min). The chloroform phase containing the crude lipid extract was removed and dried under a stream of N_2 . TAG and polar lipids were then separated by solid-phase extraction with Waters Sep-Pak columns (1 g silica cartridges, 6 mL, Waters, Ireland). Neutral lipids (TAG) were first eluted with 10 mL of 7:1 (v/v) hexane:diethyl ether; then, polar lipids were eluted with 10 mL of methanol:acetone:hexane (2:2:1 v/v/v). Solvents were then evaporated under N_2 gas, and the fatty acids were derivatized to fatty acid methyl esters (FAMES) by adding acidic methanol (3.0 mL 5% H_2SO_4 in methanol, 70°C for 3 h). FAMES were collected into hexane and quantified using a gas chromatograph equipped with a Flame Ionization Detector (SCION 436, Bruker, UK) and an Agilent CP-Wax 52CB column (Agilent Technologies, USA). Supelco 37 component standards (Sigma-Aldrich, USA) were used for identification and quantification of the FAMES. Additional standards were obtained to identify more unusual C16 and C18 series of fatty acids.

Elemental composition and protein content

The elemental composition of biomass including carbon, hydrogen, and nitrogen (CHN) was determined by elemental analysis (Elemental Microanalysis, Okehampton, UK). The protein content (%) was calculated using a nitrogen-to-protein conversion factor of $N \times 4.78$ (Lourenço et al. 2004), where N is the elemental nitrogen content (%).

Calculations

The volumetric productivity ($\text{g L}^{-1} \text{ day}^{-1}$) was calculated between two time points as in Eq. (2):

$$P_i = \frac{C_{x,i} - C_{x,i-1}}{t_i - t_{i-1}} \quad (2)$$

where P is the productivity, $C_{x,i}$ and $C_{x,i-1}$ are the concentrations of the biomass (g L^{-1}) at two time points and $t_i - t_{i-1}$ is the time (days) between measurements. For the salinity experiment, the maximum productivity was calculated between days 5 and 7. In the stress experiment, Li-Ex I and Li-Ex II, the maximum volumetric productivity occurred at different times in different treatments and was calculated as the highest productivity observed between two time points in each treatment. The maximum areal productivity P_A ($\text{g m}^{-2} \text{ day}^{-1}$) was calculated according to Eq. (3):

$$P_A = \frac{P_{\max} \cdot V_R}{I_A} \quad (3)$$

where P_{\max} is the maximum productivity ($\text{g L}^{-1} \text{ day}^{-1}$), V_R is the reactor volume (0.38 L), and I_A is illuminated surface area (0.029 m^2). The maximum biomass yield per mol photons PAR ($Y_{x/\text{mol}}$, g mol^{-1} photons) was calculated using Eq. (4).

$$Y_{x/\text{mol}} = \frac{P_A}{\text{PPFD}} \quad (4)$$

where PPFD is the average PAR photon flux density on surface of the reactor ($\text{mol photons m}^{-2} \text{ day}^{-1}$).

Statistical analysis

The statistical software R studio version 0.99 was used to perform one-way analysis of variance (ANOVA) and post-hoc Tukey's multiple comparison tests (R Core Team 2018). Data were tested for normality and homogeneity of variances using Shapiro–Wilk and Bartlett tests, respectively. P values smaller than 0.05 were considered significant, and details of each test can be found in supporting information Table 1S.

Results

Effect of salinity on growth in 100 mL bubble tubes

The growth of *K. antarctica* in different salinities ranging from freshwater (0‰) to seawater (32‰) conditions is shown in Table 2 and Fig. 1S. Higher growth rates were attained under low salinity conditions ($\leq 16‰$). At salinity levels from 0 to 16‰, the maximum dry weight was in the range 2.69 to 2.90 g L^{-1} . However, at salinity 32‰, the maximum biomass concentration was lower, reaching only 2.14 g L^{-1} . Although growth rates at salinities 2 and 4‰ were similar, the highest productivity of 0.53 $\text{g L}^{-1} \text{ day}^{-1}$ was achieved at salinity 4‰. Hence, 4‰ was selected as the optimal salinity for further cultivations.

Table 2 Maximum dry weight and biomass productivity of *K. antarctica* cultured under different salinities

Salinity (‰)	Maximum dry weight (g L ⁻¹)	Maximum productivity (g L ⁻¹ day ⁻¹)
0	2.69 ± 0.03	0.51 ± 0.006
2	2.87 ± 0.10	0.50 ± 0.001
4	2.90 ± 0.02	0.53 ± 0.042
8	2.77 ± 0.03	0.46 ± 0.026
16	2.69 ± 0.06	0.48 ± 0.002
32	2.14 ± 0.14	0.45 ± 0.052

The maximum dry weight is the highest value recorded during the 14-day cultivation period

The maximum productivity was recorded from day 5 to 7 in all treatments

Values are mean ± the standard error of duplicates

Effect of different stressors on growth in 350 mL bubble tubes

To select the best strategy that enables *K. antarctica* to produce high amounts of fatty acids and PUFAs, the impact of nitrogen (N⁻) starvation, phosphorus (P⁻) starvation, and high salinity (HS) conditions on growth, fatty acid, and protein assimilation was investigated. The growth curves of *K.*

antarctica cultivated under these conditions are shown in Fig. 2a. In all conditions, the biomass concentration increased, but there were significant differences in the maximum productivity ($F = 53.8$, $p < 0.001$) and the maximum cell density ($F = 311.5$, $p < 0.001$) among the treatments (Table 1S). Control cultures displayed strong growth and achieved the highest dry weight of 3.73 g L⁻¹ at day 5, significantly higher than each of the other treatments (Tukey's HSD, $p < 0.001$). The lag phase in the HS treatment extended to 2 days, but the maximum growth rate of 0.69 g L⁻¹ day⁻¹ was slightly higher than the 0.57 g L⁻¹ day⁻¹ recorded in P-starved conditions, and eventually both achieved comparable maximum cell densities of 2.23 and 2.30 g L⁻¹, respectively (Tukey's HSD, $p = 0.857$). The maximum productivity of *K. antarctica* under N starvation was however significantly lower than each of the other treatments (Tukey's HSD, $p < 0.001$), and the maximum cell density reached only a quarter of that achieved in the control medium (Table 3).

Figure 2b,d illustrates the nitrate and phosphate assimilation capacity of *K. antarctica* under the different stress conditions, while the corresponding nutrient uptake rates are presented in Table 3. Concordant with the growth rates, there were also significant differences in nitrate uptake ($F = 47.0$, $p < 0.001$) and phosphate uptake ($F = 33.62$, $p < 0.001$) between the treatments. Phosphate uptake in the N-starved

Fig. 2 Effect of N starvation, P starvation, and high salinity (32‰) on the growth and nutrient uptake of *K. antarctica* in batch cultures. **a** Cell density (g L⁻¹). **b** Extracellular nitrate concentration (mM). **c** Absorbance ratio (A_{680}/A_{540}). **d** Extracellular phosphate concentration (mM). The error bars indicate standard error of the mean ($n = 3$)

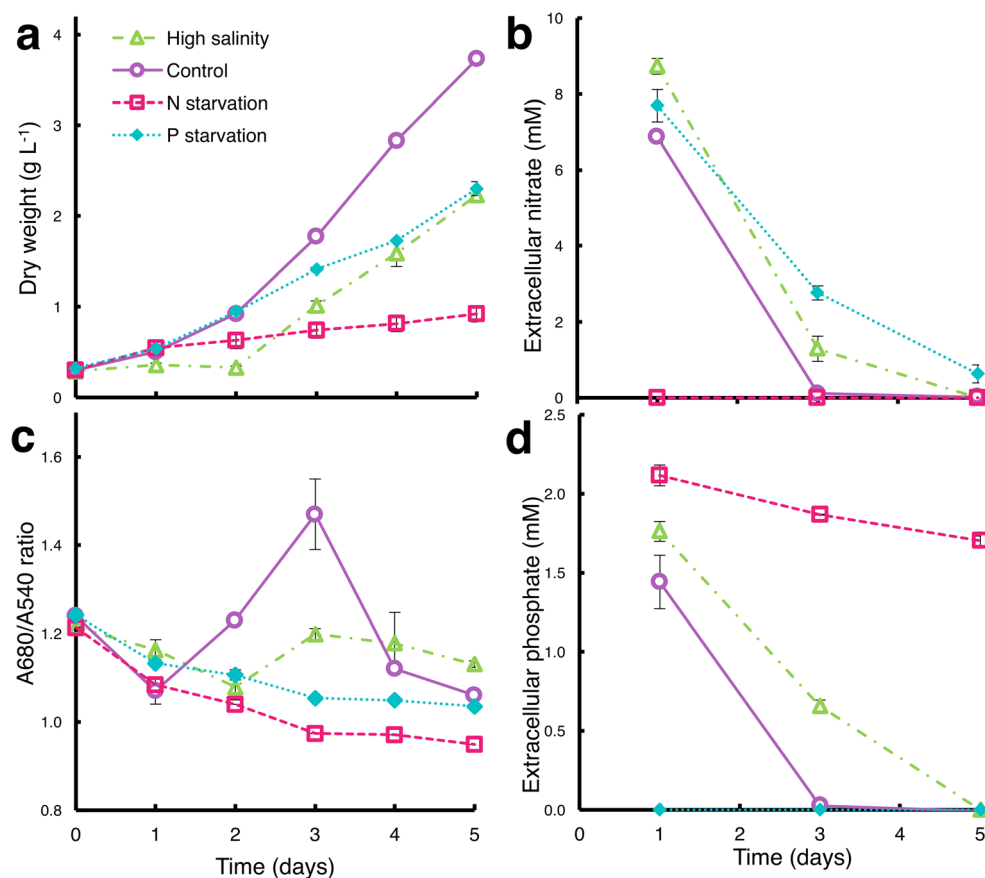


Table 3 Effect of N starvation, P starvation, and high salinity (32‰) on growth, biochemical composition, and nutrient assimilation. The maximum biomass productivities (P_v) ($\text{g L}^{-1} \text{ day}^{-1}$), maximum cell density (g L^{-1}), fatty acid content per volume of culture (Y_{FA}) (mg L^{-1}), nitrate uptake ($\text{mM L}^{-1} \text{ day}^{-1}$), and phosphate uptake ($\text{mM L}^{-1} \text{ day}^{-1}$) were calculated as described in the “Materials and methods” section. Maximum cell density (g L^{-1}), fatty acid content (C_{FA}) (% DW), protein content (C_{PRO}) (% DW), and the C:N ratio were measured at day 5

Treatment	Maximum P_v ($\text{g L}^{-1} \text{ day}^{-1}$)	Maximum cell density (g L^{-1}) (day 5)	Y_{FA} (mg L^{-1}) (day 5)	C_{FA} (% DW) (day 5)	C_{PRO} (% DW) (day 5)	C:N ratio (day 5)	Nitrate uptake ($\text{mM L}^{-1} \text{ day}^{-1}$)	Phosphate uptake ($\text{mM L}^{-1} \text{ day}^{-1}$)
Control	1.06 ± 0.05	3.73 ± 0.07	507.6 ± 38.4	13.6 ± 0.8	21.9 ± 0.7	10.72 ± 0.34	3.38 ± 0.08	0.71 ± 0.08
N-	0.24 ± 0.02	0.92 ± 0.01	165.4 ± 2.5	17.9 ± 0.2	12.2 ± 0.2	19.80 ± 0.37	–	0.12 ± 0.03
P-	0.57 ± 0.07	2.30 ± 0.08	411.5 ± 29.0	17.8 ± 0.7	31.4 ± 0.1	7.94 ± 0.04	2.46 ± 0.12	–
HS	0.69 ± 0.03	2.23 ± 0.08	241.5 ± 12.6	10.8 ± 0.5	27.0 ± 0.7	7.95 ± 0.26	3.72 ± 0.07	0.55 ± 0.03

cultures was $0.12 \text{ mM L}^{-1} \text{ day}^{-1}$, which was significantly lower than the uptake rate of $0.71 \text{ mM L}^{-1} \text{ day}^{-1}$ in the control cultures and $0.55 \text{ mM L}^{-1} \text{ day}^{-1}$ in the HS treatments (Tukey’s HSD, $p \leq 0.003$). The rate of nitrate uptake in P-starved cultures was $2.46 \text{ mM L}^{-1} \text{ day}^{-1}$, which was significantly lower than that of the control ($3.38 \text{ mM L}^{-1} \text{ day}^{-1}$) and HS groups ($3.72 \text{ mM L}^{-1} \text{ day}^{-1}$) (Tukey’s HSD, $p < 0.001$). Due to rapid growth in the control treatments, nitrate and phosphate were each exhausted at day 3 (Fig. 2b,d). Similarly, the HS treatments also consumed the available nitrate by day 5. Hence, *K. antarctica* in the control medium and HS conditions still experienced N + P and N starvation, respectively, during the later stages of cultivation.

The A_{680}/A_{540} ratio in both N- and P-starved media decreased throughout the experiment, but N-starved cells were characterized by lower ratios than P-starved cells, indicating more substantial loss of photosynthetic pigments (Fig. 2c). At the end of cultivation, the values for N-starved and P-starved cells were 0.95 and 1.04, respectively. Control cultures were characterized by an initial increase in A_{680}/A_{540} , reaching 1.47 at day 3, followed by a decline to 1.06 at day 5. This pattern is concordant with increased mutual shading during growth, followed by the effects of nutrient availability during the later stages of cultivation.

Effect of different stressors on fatty acid and protein production in 350 mL bubble tubes

The effects of N, P, and HS stress on the total fatty acid contents (C_{FA} , % DW) are shown in Table 3. There were significant differences in C_{FA} between the treatments ($F = 33.9$, $p < 0.001$), where both N- and P- conditions yielded significantly higher fatty acid concentrations (each 18% DW) than control and HS conditions (Tukey’s HSD, $p \leq 0.004$). However, the reduced biomass productivity under N starvation ultimately led to the lowest overall fatty acid yield (Y_{FA}) of 165.4 mg L^{-1} in this treatment. In contrast, the control cultures achieved the highest Y_{FA} of 507.6 mg L^{-1} .

In all treatments, the total fatty acid content increased from day 2 to day 5, mainly due to TAG accumulation (Table 4). The highest proportion of TAG was detected under N starvation at day 5, where it accounted for 79.5% of TFA ($179.1 \text{ mg g}^{-1} \text{ DW}$). In nutrient-replete conditions (control, day 2), the dominant fatty acids were C16:0, C16:4n-3, C18:3n-3 (α -linolenic acid, ALA), and C20:5n-3 (EPA). However, under N- and P-starved conditions, C16:0, C18:1n-9 (oleic acid, OA), C18:2n-6 (linoleic acid, LA), and ALA became dominant. TAG accumulation was attributed predominantly to a large increase in OA, comprising up to 52.7% of neutral lipids. However, the PUFAs LA, ALA, and C20:4n-6 (arachidonic acid, ARA) were also enriched in TAG, and together total PUFAs accounted for 33.9–45.8% of TAG at day 5 (Table 4).

Table 4 Total fatty acids (TFA) and fatty acids in TAG under N starvation, P starvation, and HS (32%) conditions (mg g⁻¹ DW)

	Control						N-						P-						HS						
	Day 2		Day 5		Day 2		Day 5		Day 2		Day 5		Day 2		Day 5		Day 2		Day 5		Day 2		Day 5		
	TFA	TAG	TFA	TAG	TFA	TAG	TFA	TAG	TFA	TAG	TFA	TAG	TFA	TAG	TFA	TAG	TFA	TAG	TFA	TAG	TFA	TAG	TFA	TAG	
C14:0	0.54 (0.05)	0.04 (0.01)	1.17 (0.03)	0.38 (0.04)	0.28 (0.03)	0.46 (0.17)	0.46 (0.17)	0.28 (0.03)	1.13 (0.06)	0.55 (0.01)	0.41 (0.09)	0.41 (0.09)	1.26 (0.06)	0.11 (0.03)	0.58 (0.03)	0.31 (0.08)	0.31 (0.08)	0.02 (0.02)	1.14 (0.06)	0.02 (0.02)	1.26 (0.06)	0.11 (0.03)	0.58 (0.03)	0.31 (0.08)	0.31 (0.08)
C16:0	3.62 (0.28)	0.36 (0.03)	19.16 (1.30)	10.71 (1.17)	5.31 (0.74)	7.42 (1.04)	7.42 (1.04)	5.31 (0.74)	17.23 (0.50)	11.47 (0.27)	6.66 (0.96)	6.66 (0.96)	19.24 (1.90)	2.20 (0.19)	7.21 (0.22)	3.19 (0.81)	3.19 (0.81)	1.39 (0.21)	16.51 (1.02)	1.39 (0.21)	19.24 (1.90)	2.20 (0.19)	7.21 (0.22)	3.19 (0.81)	3.19 (0.81)
C16:2 (n-6)	0.64 (0.06)	0.05 (0.02)	6.56 (0.04)	2.04 (0.12)	0.79 (0.11)	2.57 (0.26)	2.57 (0.26)	0.79 (0.11)	4.43 (0.22)	1.99 (0.06)	1.57 (0.17)	1.57 (0.17)	6.42 (0.33)	0.37 (0.05)	2.71 (0.08)	0.61 (0.08)	0.61 (0.08)	0.12 (0.01)	5.48 (0.34)	0.12 (0.01)	6.42 (0.33)	0.37 (0.05)	2.71 (0.08)	0.61 (0.08)	0.61 (0.08)
C16:3 (n-3)	1.69 (0.09)	0.16 (0.02)	5.48 (0.07)	2.11 (0.13)	1.72 (0.22)	5.04 (0.46)	5.04 (0.46)	1.72 (0.22)	6.97 (0.30)	3.87 (0.13)	3.82 (0.50)	3.82 (0.50)	7.79 (0.40)	0.94 (0.13)	4.11 (0.09)	1.63 (0.24)	1.63 (0.24)	0.23 (0.03)	5.31 (0.29)	0.23 (0.03)	7.79 (0.40)	0.94 (0.13)	4.11 (0.09)	1.63 (0.24)	1.63 (0.24)
C16:4 (n-3)	6.16 (0.32)	1.35 (0.08)	5.14 (0.11)	2.42 (0.12)	1.22 (0.17)	3.36 (0.33)	3.36 (0.33)	1.22 (0.17)	3.87 (0.17)	2.14 (0.09)	4.59 (0.59)	4.59 (0.59)	4.89 (0.19)	1.41 (0.19)	2.76 (0.09)	3.79 (0.66)	3.79 (0.66)	0.72 (0.09)	5.03 (0.35)	0.72 (0.09)	4.89 (0.19)	1.41 (0.19)	2.76 (0.09)	3.79 (0.66)	3.79 (0.66)
C18:0	0.32 (0.14)	0.29 (0.15)	1.61 (0.54)	0.48 (0.22)	0.00 (0.00)	0.00 (0.00)	0.00 (0.00)	0.00 (0.00)	1.61 (0.44)	0.60 (0.08)	0.00 (0.00)	0.00 (0.00)	2.47 (0.64)	0.00 (0.00)	0.62 (0.11)	0.00 (0.10)	0.00 (0.10)	0.00 (0.00)	2.11 (0.34)	0.00 (0.00)	2.47 (0.64)	0.00 (0.00)	0.62 (0.11)	0.00 (0.10)	0.00 (0.10)
C18:1 (n-9)	0.53 (0.03)	0.13 (0.01)	37.03 (3.82)	32.85 (3.96)	23.74 (3.24)	25.20 (3.37)	25.20 (3.37)	23.74 (3.24)	78.78 (2.07)	75.05 (2.45)	7.71 (0.71)	7.71 (0.71)	57.56 (2.03)	6.34 (0.56)	52.69 (1.96)	2.43 (0.34)	2.43 (0.34)	1.86 (0.26)	22.55 (0.49)	1.86 (0.26)	57.56 (2.03)	6.34 (0.56)	52.69 (1.96)	2.43 (0.34)	2.43 (0.34)
C18:1 (n-7)	0.24 (0.01)	0.00 (0.00)	1.09 (0.05)	0.65 (0.05)	0.35 (0.05)	0.51 (0.06)	0.51 (0.06)	0.35 (0.05)	1.31 (0.03)	1.01 (0.03)	0.50 (0.05)	0.50 (0.05)	2.18 (0.13)	0.26 (0.03)	1.44 (0.07)	0.13 (0.04)	0.13 (0.04)	0.02 (0.02)	0.58 (0.05)	0.02 (0.02)	2.18 (0.13)	0.26 (0.03)	1.44 (0.07)	0.13 (0.04)	0.13 (0.04)
C18:2 (n-6) (LA)	1.55 (0.06)	0.17 (0.01)	20.45 (0.74)	11.34 (1.04)	5.71 (0.79)	8.92 (1.08)	8.92 (1.08)	5.71 (0.79)	20.63 (0.32)	15.44 (0.55)	6.57 (0.71)	6.57 (0.71)	27.05 (1.05)	2.97 (0.32)	16.75 (0.51)	2.02 (0.29)	2.02 (0.29)	0.94 (0.13)	15.74 (0.77)	0.94 (0.13)	27.05 (1.05)	2.97 (0.32)	16.75 (0.51)	2.02 (0.29)	2.02 (0.29)
C18:3 (n-6)	0.47 (0.04)	0.13 (0.01)	2.93 (0.09)	1.78 (0.13)	1.50 (0.20)	2.13 (0.27)	2.13 (0.27)	1.50 (0.20)	4.29 (0.07)	3.76 (0.12)	2.56 (0.32)	2.56 (0.32)	8.90 (0.49)	0.98 (0.13)	4.45 (0.11)	0.52 (0.08)	0.52 (0.08)	0.26 (0.03)	2.27 (0.08)	0.26 (0.03)	8.90 (0.49)	0.98 (0.13)	4.45 (0.11)	0.52 (0.08)	0.52 (0.08)
C18:3 (n-3) (ALA)	11.46 (0.64)	1.50 (0.11)	16.80 (0.36)	7.49 (0.54)	5.61 (0.66)	12.94 (1.28)	12.94 (1.28)	5.61 (0.66)	19.85 (0.72)	11.63 (0.48)	12.98 (1.66)	12.98 (1.66)	22.66 (0.93)	4.45 (0.57)	13.46 (0.40)	8.43 (1.33)	8.43 (1.33)	1.87 (0.24)	16.94 (1.03)	1.87 (0.24)	22.66 (0.93)	4.45 (0.57)	13.46 (0.40)	8.43 (1.33)	8.43 (1.33)
C18:4 (n-3)	2.52 (0.15)	0.76 (0.05)	1.79 (0.04)	0.93 (0.05)	0.40 (0.06)	0.75 (0.08)	0.75 (0.08)	0.40 (0.06)	0.98 (0.04)	0.63 (0.02)	2.14 (0.31)	2.14 (0.31)	2.85 (0.11)	0.85 (0.13)	1.92 (0.04)	1.35 (0.24)	1.35 (0.24)	0.37 (0.05)	1.87 (0.12)	0.37 (0.05)	2.85 (0.11)	0.85 (0.13)	1.92 (0.04)	1.35 (0.24)	1.35 (0.24)
C20:1 (n-9)	0.46 (0.02)	0.00 (0.00)	5.09 (0.38)	3.09 (0.38)	1.81 (0.24)	2.65 (0.34)	2.65 (0.34)	1.81 (0.24)	6.84 (0.10)	5.52 (0.20)	1.18 (0.10)	1.18 (0.10)	4.90 (0.17)	0.82 (0.05)	3.91 (0.13)	0.77 (0.13)	0.77 (0.13)	0.28 (0.03)	3.80 (0.12)	0.28 (0.03)	4.90 (0.17)	0.82 (0.05)	3.91 (0.13)	0.77 (0.13)	0.77 (0.13)
C20:4 (n-6) (ARA)	1.42 (0.09)	0.55 (0.03)	4.79 (0.17)	2.54 (0.18)	2.20 (0.33)	3.19 (0.41)	3.19 (0.41)	2.20 (0.33)	7.37 (0.05)	5.74 (0.18)	1.72 (0.22)	1.72 (0.22)	4.63 (0.17)	1.12 (0.16)	3.29 (0.10)	1.06 (0.17)	1.06 (0.17)	0.58 (0.05)	3.61 (0.15)	0.58 (0.05)	4.63 (0.17)	1.12 (0.16)	3.29 (0.10)	1.06 (0.17)	1.06 (0.17)
C20:5 (n-3) (EPA)	3.74 (0.25)	1.70 (0.12)	6.71 (0.17)	4.37 (0.21)	2.07 (0.28)	2.83 (0.35)	2.83 (0.35)	2.07 (0.28)	3.78 (0.01)	3.03 (0.08)	3.01 (0.37)	3.01 (0.37)	5.44 (0.15)	2.07 (0.27)	4.08 (0.08)	2.06 (0.35)	2.06 (0.35)	1.18 (0.17)	5.42 (0.20)	1.18 (0.17)	5.44 (0.15)	2.07 (0.27)	4.08 (0.08)	2.06 (0.35)	2.06 (0.35)
Σ SFA	4.48 (0.22)	0.68 (0.19)	21.94 (1.87)	11.57 (1.39)	5.82 (0.82)	7.73 (1.29)	7.73 (1.29)	5.82 (0.82)	19.98 (0.86)	12.62 (0.26)	7.03 (1.09)	7.03 (1.09)	22.98 (2.51)	2.62 (0.20)	8.41 (0.13)	3.34 (1.05)	3.34 (1.05)	1.43 (0.26)	19.75 (1.42)	1.43 (0.26)	22.98 (2.51)	2.62 (0.20)	8.41 (0.13)	3.34 (1.05)	3.34 (1.05)

Table 4 (continued)

	Control						N-						P-						HS					
	Day 2		Day 5		Day 2		Day 5		Day 2		Day 5		Day 2		Day 5		Day 2		Day 5		Day 2		Day 5	
	TFA	TAG	TFA	TAG	TFA	TAG	TFA	TAG	TFA	TAG	TFA	TAG	TFA	TAG	TFA	TAG	TFA	TAG	TFA	TAG	TFA	TAG	TFA	TAG
Σ MUFA	1.23 (0.03)	0.13 (0.01)	51.68 (4.23)	36.59 (4.39)	28.36 (3.77)	25.90 (3.54)	86.92 (2.14)	81.58 (2.68)	9.39 (0.86)	7.42 (0.63)	64.64 (2.27)	58.03 (2.15)	3.33 (0.50)	2.16 (0.30)	26.93 (0.61)	21.53 (0.33)								
Σ PUFA	29.65 (1.68)	6.38 (0.45)	73.75 (1.56)	35.02 (2.48)	41.73 (4.50)	21.21 (2.79)	72.17 (1.63)	48.24 (1.62)	38.96 (4.82)	15.18 (1.94)	90.64 (3.80)	53.52 (1.48)	21.47 (3.43)	6.26 (0.78)	61.68 (3.11)	24.95 (0.57)								
Σ LC-PUFA	5.16 (0.34)	2.24 (0.15)	12.03 (0.28)	6.92 (0.38)	6.01 (0.76)	4.28 (0.59)	11.15 (0.06)	8.77 (0.25)	4.73 (0.59)	3.20 (0.44)	10.07 (0.32)	7.36 (0.18)	3.13 (0.52)	1.76 (0.23)	9.03 (0.25)	5.45 (0.03)								
ω-3 fatty acids	25.57 (1.45)	4.40 (0.17)	35.92 (0.66)	17.33 (1.03)	24.92 (2.49)	11.02 (1.37)	35.46 (1.21)	21.30 (0.78)	26.55 (3.42)	9.73 (1.28)	43.64 (1.78)	26.32 (0.69)	17.26 (2.82)	4.37 (0.57)	34.58 (1.95)	13.27 (0.43)								
ω-6 fatty acids	4.08 (0.23)	0.90 (0.07)	34.72 (0.97)	17.69 (1.47)	16.81 (2.01)	10.20 (1.41)	36.71 (0.46)	26.94 (0.86)	12.42 (1.40)	5.45 (0.65)	47.00 (2.02)	27.19 (0.79)	4.21 (0.62)	1.89 (0.22)	27.09 (1.16)	11.69 (0.14)								
ω-3/ω-6 ratio	6.27 (0.01)	4.99 (0.62)	1.04 (0.02)	0.98 (0.03)	1.49 (0.03)	1.09 (0.02)	0.97 (0.02)	0.79 (0.01)	2.13 (0.04)	1.78 (0.02)	0.93 (0.00)	0.97 (0.00)	4.08 (0.11)	2.30 (0.05)	1.27 (0.02)	1.13 (0.02)								
Total fatty acids	35.36 (1.84)	7.20 (0.27)	135.80 (7.65)	83.18 (8.22)	77.82 (9.53)	52.94 (7.15)	179.08 (2.10)	142.44 (4.51)	55.38 (6.76)	25.22 (2.76)	178.25 (7.29)	119.96 (3.73)	28.14 (4.96)	9.86 (1.32)	108.36 (4.97)	54.54 (0.83)								

Mean values (±standard error) of triplicates per treatment are given in the table
 A standard error of 0.00 indicates that the standard error was less than 0.005 mg g⁻¹

The highest PUFA content of 90.6 mg g⁻¹ DW, as well as the highest ω-3 fatty acid content of 43.6 mg g⁻¹ DW, was observed after 5 days of P starvation. The LA and ALA contents of P-starved cells amounted to 27.1 and 22.7 mg g⁻¹ DW, respectively, which were also higher than the other treatments. The HS treatment induced the accumulation of TAG with a large proportion of OA at day 2. The proportion of TAG was higher in the HS treatment (35.0% TFA) than that of control cultures (20.2% TFA) at day 2.

The highest amount of EPA was 6.7 mg g⁻¹ DW (4.9% TFA) in high-density control cultures (day 5) but slightly lower during P and N starvation at 5.4 and 3.8 mg g⁻¹ DW, respectively (Table 4). The lowest EPA content of 2.1 mg g⁻¹ DW was recorded for the HS group at day 2. In contrast to EPA, the total ARA content was enhanced by N starvation. ARA increased from 1.4 mg g⁻¹ DW in nutrient-replete conditions to 7.4 and 4.6 mg g⁻¹ DW (4.1 and 2.6% TFA) in N and P treatments, respectively, primarily accumulating in the TAG fraction.

The total protein content (C_{PRO}) also varied significantly between the different treatments ($F = 269.9, p < 0.001$). Under P starvation, the protein content of *K. antarctica* at day 5 was 31.4% DW, which was significantly higher than that of N- (12.2% DW), HS (27.0% DW), and control treatments (21.9% DW) (Tukey's HSD, $p \leq 0.001$). Cells in N-starved conditions therefore had the highest C:N ratio of 19.8, approximately twice that of the other treatments, which ranged from 7.9 to 10.7 (Table 3).

Effect of light intensity on growth in 380 mL flat-plate photobioreactors

The effect of light intensity on the growth of *K. antarctica* was studied in flat-plate photobioreactors. In the first experiment (Li-Ex I), the maximum biomass productivity increased from 0.48 to 1.04 g L⁻¹ day⁻¹ when the PPFD was raised from 70 to 250 μmol photons m⁻² s⁻¹, but there was no further increase in growth rate when light was increased to 500 μmol photons m⁻² s⁻¹ (Table 5, Fig. 3a). The extracellular

nitrate in all cultures was exhausted by day 8 (Fig. 3c). In cultures supplied with 250 and 500 μmol photons m⁻² s⁻¹, the A₆₈₀/A₅₄₀ ratio decreased rapidly after day six, reaching 0.95 to 0.93 after nine days. In cultures supplied with 70 μmol photons m⁻² s⁻¹ though, the effect was dampened, and the A₆₈₀/A₅₄₀ ratio reached a lowest value of 0.98 at day 16 (Fig. 3b). Under all light conditions, the initial pH 6.5 increased to pH 7.8–7.9 by day 7 or 8, then decreased slightly to pH 7.6–7.7 toward the end of cultivation, as the growth rate slowed (Fig. 3d). Together, the attenuated growth under 500 μmol photons m⁻² s⁻¹ coupled with the nitrate and pH data (Table 5) indicated that nutrient availability and possibly CO₂ supply might have constrained the maximum growth rate. To test whether we could obtain higher yields, the nutrient and CO₂ concentrations were subsequently increased and the experiment was repeated at 500 μmol photons m⁻² s⁻¹. In this second experiment (Li-Ex II), the maximum biomass productivity was indeed substantially higher, reaching a maximum of 2.37 g L⁻¹ day⁻¹, with the highest cell density measured at 11.68 g L⁻¹ at the end of cultivation (Fig. 4c, Table 5). In Li-Ex II, the absorbance ratio A₆₈₀/A₅₄₀ remained stable between 0.95 and 1.09 throughout the experiments.

Photosynthetic yield in 380 mL flat-plate photobioreactors

To characterize the photosynthetic efficiency of *K. antarctica* under different light intensities, the maximum biomass yield per mol photons PAR ($Y_{x/mol}$, g mol⁻¹ photons) was calculated for each treatment (Table 5). The cultures under low irradiance used light more efficiently than those at higher light intensities, averaging 1.05 g mol⁻¹ photons at 70 μmol photons m⁻² s⁻¹, and reducing to 0.27 g mol⁻¹ photons at 500 μmol photons m⁻² s⁻¹. In Li-Ex II, however, *K. antarctica* showed improved response at 500 μmol photons m⁻² s⁻¹, with strong growth throughout the duration of the experiment (Fig. 4a). In this second experiment, the photosynthetic efficiency at 500 μmol photons m⁻² s⁻¹ was improved to 0.73 g mol⁻¹ photons, and the maximum areal productivity of 31.58 g m⁻² day⁻¹ was the highest recorded (Table 5).

Table 5 Biomass production of *K. antarctica* grown in flat-plate photobioreactors at a photosynthetic photon flux density (PPFD) of 70, 250, or 500 μmol photons m⁻² s⁻¹. Values are the maximum biomass

productivity, maximum areal productivity, and maximum photosynthetic yield obtained from the experiments Li-Ex I and Li-Ex II

Medium	PPFD (μmol m ⁻² s ⁻¹)	CO ₂ (%)	Max productivity (g L ⁻¹ day ⁻¹)	Max areal productivity (g m ⁻² day ⁻¹)	Max biomass yield light (g mol ⁻¹ photons)
2N-BBM	70	1	0.48 ± 0.01	6.36 ± 0.08	1.052 ± 0.014
2N-BBM	250	1	1.04 ± 0.01	13.85 ± 0.07	0.641 ± 0.003
2N-BBM	500	1	0.87 ± 0.10	11.62 ± 1.39	0.269 ± 0.032
3× 3N-BBM	500	5	2.37 ± 0.09	31.58 ± 1.21	0.731 ± 0.028

Mean values (±standard error) of duplicates per treatment are given in the table

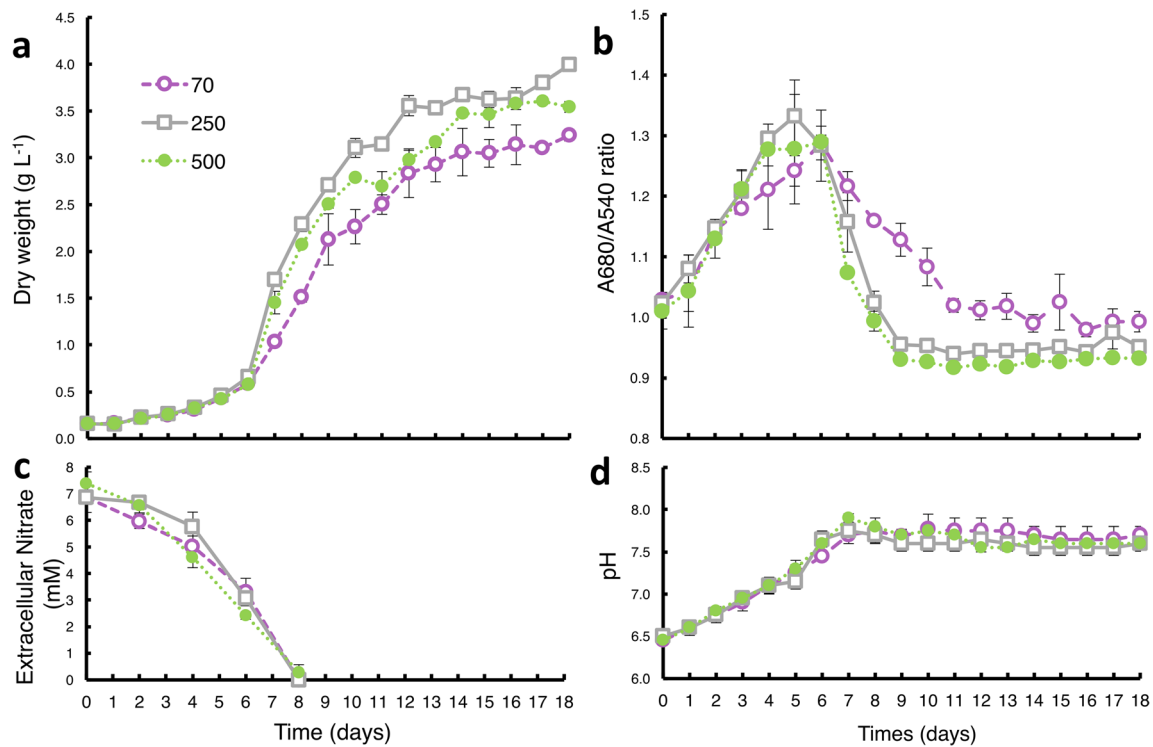


Fig. 3 The effect of the photosynthetic photon flux density (70, 250, and 500 $\mu\text{mol photons m}^{-2} \text{s}^{-1}$) on the growth of *K. antarctica* in flat-plate photobioreactors over 18 days. **a** Cell density (g L^{-1}). **b** Extracellular

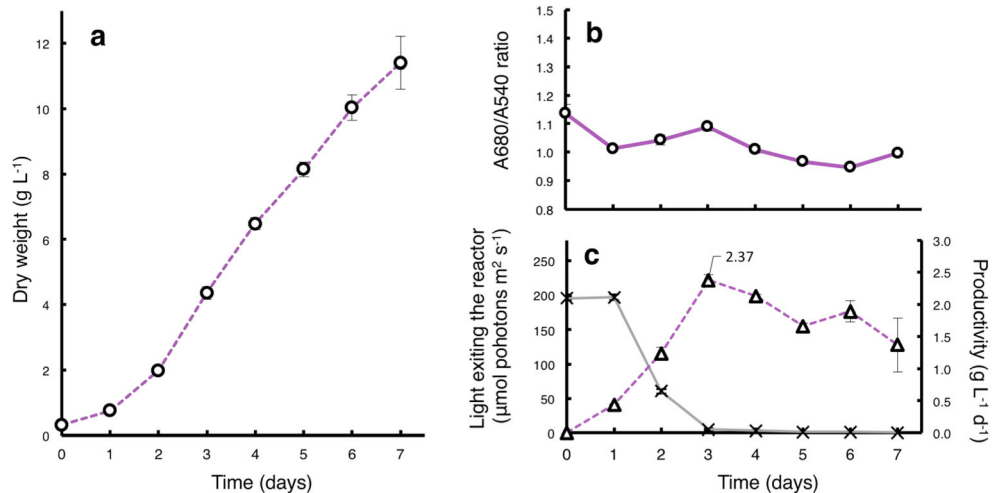
nitrate concentration (mM). **c** The absorbance ratio A_{680}/A_{540} . **d** The culture pH. The error bars indicate the standard error of duplicate cultivations

Fatty acid production in 380 mL flat-plate photobioreactors

In the flat-plate photobioreactors, *K. antarctica* illuminated with 70, 250, and 500 $\mu\text{mol photons m}^{-2} \text{s}^{-1}$ was able to accumulate considerable amounts of fatty acids, with a large increase in TAG and a slight decrease in polar lipid fatty acids toward the stationary phase (Fig. 5, Fig. 2S). The highest TFA content of 271.9 mg g^{-1} DW was recorded under 250 $\mu\text{mol photons m}^{-2} \text{s}^{-1}$ at day 18, where 90.1% TFA was

found in TAG (Fig. 2S). Total PUFAs at day 10 (late exponential phase) ranged from 52.9 to 53.9 mg g^{-1} DW and consistently increased up to 88.5 mg g^{-1} DW at day 18 in the late stationary phase. The highest total PUFA content was recorded at day 18 when cultures were supplied with 250 $\mu\text{mol photons m}^{-2} \text{s}^{-1}$, where 86.2% of total PUFAs were found in TAG. In all Li-Ex I treatments, a time-dependent increase in ARA and LA content was observed, mostly in the TAG fraction (Fig. 5a,b). The highest ARA content was obtained under 250 $\mu\text{mol photons m}^{-2} \text{s}^{-1}$ at 9.6 mg g^{-1} DW

Fig. 4 Growth of *K. antarctica* in optimized conditions in flat-plate photobioreactors (Li-Ex II, 500 $\mu\text{mol photons m}^{-2} \text{s}^{-1}$), using increased amounts of nutrients ($3 \times 3\text{N-BBM}$) and CO_2 concentration (5% $\text{CO}_2 \text{ v/v}$). **a** Cell density (g L^{-1}). **b** Absorbance ratio, A_{680}/A_{540} . **c** Light transmitted through the reactor vessel ($\mu\text{mol photons m}^{-2} \text{s}^{-1}$) and biomass productivity ($\text{g L}^{-1} \text{day}^{-1}$). Error bars indicate the standard error of the mean ($n = 2$)



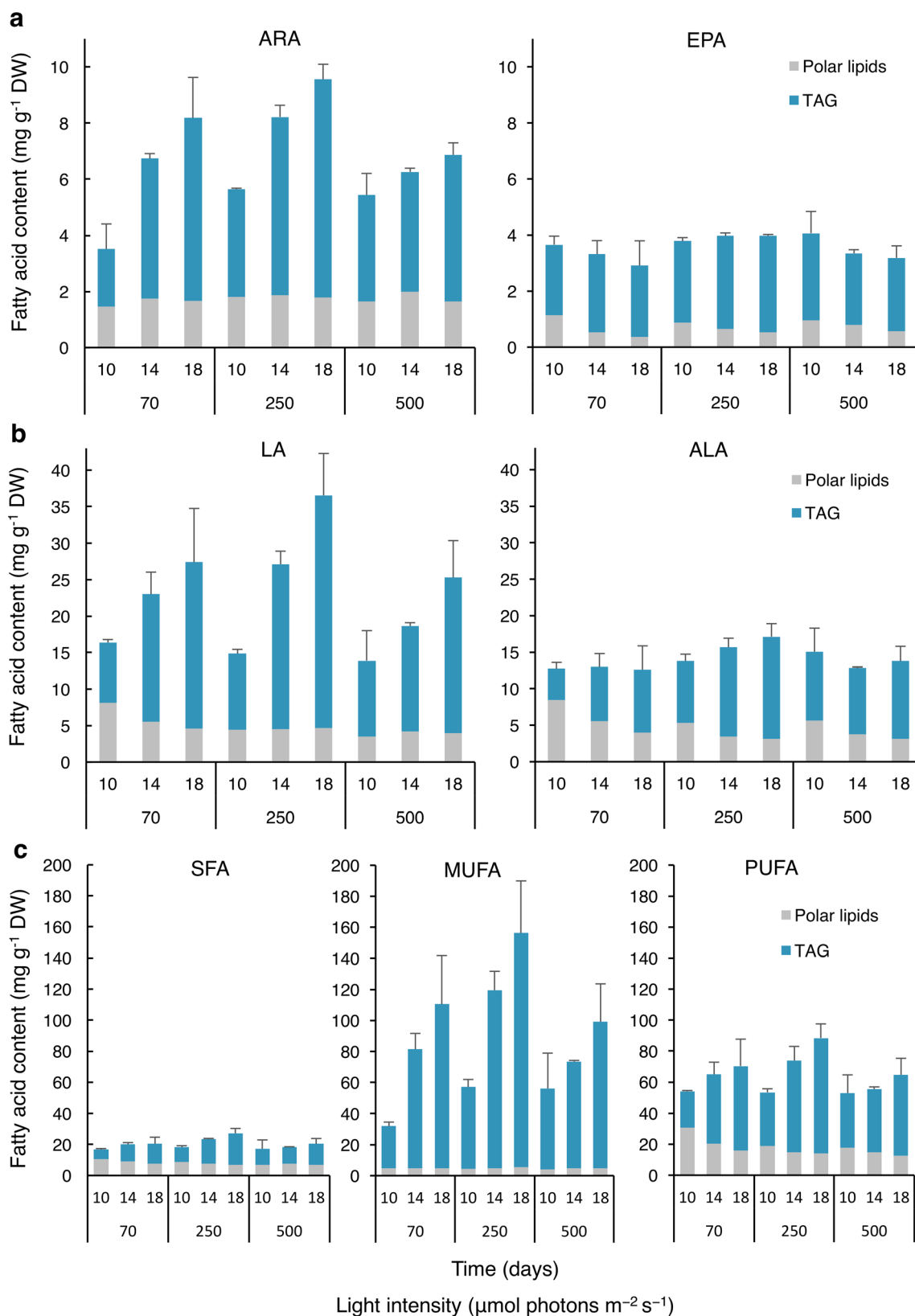


Fig. 5 The fatty acid composition (mg g^{-1} DW) of TAG and polar lipids from *K. antarctica* grown in flat-plate photobioreactors under different light intensities (70, 250, and $500 \mu\text{mol photons m}^{-2} \text{s}^{-1}$), determined at days 10, 14, and 18. **a** Arachidonic acid, C₂₀:4n-6 (ARA, left) and eicosapentaenoic

acid, C₂₀:5n-3 (EPA, right). **b** Linoleic acid (LA, left) and α -linolenic acid (ALA, right). **c** Saturated fatty acids (SFA, left), monounsaturated fatty acids (MUFA, center), and polyunsaturated fatty acids (PUFA, right). Error bars indicate the standard error of duplicate cultivations

(3.5% TFA) in the late stationary phase. The total EPA content was mostly conserved throughout growth, ranging between 2.9 and 4.1 mg g⁻¹ DW (Fig. 5a). However, the percent share of EPA consistently decreased from 3.6% of TFA during the late exponential phase to its lowest value of 1.5% of TFA in the late stationary phase. The ratio of ω -3 to ω -6 fatty acids was the highest at day 10, but it decreased thereafter to 0.5, irrespective of the PPF (Fig. 2S), due to a large increase in the abundance of LA (Fig. 5b).

Discussion

This study aimed to investigate and optimize the growth and PUFA production of the cold-adapted microalga *K. antarctica* at a cool temperature of 15 °C. Although some data is available for this strain (Vona et al. 2004; Ferroni et al. 2007; Lang et al. 2011; La Rocca et al. 2015), the results of our study present a comprehensive analysis of its growth and fatty acid profile in laboratory-scale photobioreactors. Especially, we were able to obtain relatively high biomass productivity and identify the effects of nitrogen starvation, phosphorus starvation, high salinity, and light intensity on the dynamics of PUFA and TAG production.

Salinity tolerance of *Koliella antarctica*

Salinity can affect the growth of microalgae by altering the biochemical composition and photosynthetic performance (von Alvensleben et al. 2016). To improve biomass productivity, the salinity should be optimized for each strain (Martínez-Roldán et al. 2014). Batch growth in bubble tubes indicated that *K. antarctica* preferred lower salinity conditions, with maximum growth rates obtained at 4‰. However, the microalga was euryhaline and tolerated salinities from freshwater up to natural seawater concentrations (0–32‰). Although *K. antarctica* was isolated from the Ross Sea, Antarctica (Andreoli et al. 1998), based on morphological and physiological traits, it has been suggested that the isolate could have originated from Antarctic freshwater habitats (Andreoli et al. 2000; Ferroni et al. 2007). This microalga is not found in the open seas, and our data suggests the association of *K. antarctica* with freshwater or brackish habitats. However, this does not exclude the possibility that *K. antarctica* inhabits coastal or littoral marine environments. The broad salinity tolerance of this strain offers flexibility in mass cultivation, where saline or brackish water could be used to help reduce the freshwater footprint linked to microalgae cultivation (Guieysse et al. 2013). Furthermore, the tolerance to salinity variation may also help to avoid significant decreases in outdoor productivity or culture collapse caused by evaporation or rainfall (Ishika et al. 2017).

Fatty acid production by *Koliella antarctica*

Nitrogen starvation is often the most effective strategy to trigger fatty acid accumulation in microalgae, while phosphorus starvation typically has more limited effects (Chen et al. 2017). Salinity can also be manipulated to induce fatty acid accumulation (Pal et al. 2011; Salama el et al. 2013). However, each of these stress conditions often decreases or arrests growth, which results in lower overall fatty acid productivity (Procházková et al. 2014). Here, phosphorus-starved cultures yielded similar fatty acid concentrations to nitrogen-starved cultures (each approximately 18% DW), but the reduced growth in N-starved cultures led to lower TFA yields of only 165.4 mg L⁻¹. Although this result indicates that P starvation could be an effective strategy to increase the fatty acid concentrations in this strain, the profile of nutritionally valuable PUFAs is also a criterion for bioprocess optimization.

To investigate the impact of different stressors on the fatty acid profile, total lipids were fractionated into neutral lipids (TAG) and polar (membrane) lipids. Although TAG accumulation is mostly studied for biofuel purposes (Hu et al. 2008), its importance as a valuable source of fatty acids in nutrition applications has also been recognized (Klok et al. 2014). *Koliella antarctica* accumulated TAG up to 90.0% of TFA (Li-Ex I), and, although TAG was mostly comprised of the mono-unsaturated fatty acid OA, PUFAs were also abundant and together accounted for 30.3–45.8% of TAG. This trend is similar to our previous study, where Arctic snow algae deposited comparable amounts of PUFAs in neutral lipids (Hulatt et al. 2017). Similar incorporation of PUFAs, including LC-PUFAs, into TAG has also been reported in *Thalassiosira pseudonana* and *Pavlova lutheri* (Tonon et al. 2002; Guiheneuf and Stengel 2013). *Lobosphaera incisa*, a green microalga isolated from an alpine environment, is also known to accumulate large amounts of ARA in TAG. For some microalgae that inhabit harsh environments, TAG might serve as a depot of PUFAs (Bigogno et al. 2002), and these strains could be cultivated under adverse conditions to maximize PUFA production.

For animal and human health, foods with a high ω -3 fatty acid content are desirable (Abedi and Sahari 2014). In addition, a balanced ω -3/ ω -6 ratio is also important, because ω -3 and ω -6 fatty acids and their derivatives are often functionally and metabolically antagonistic (Glencross 2009; Simopoulos 2016). The recommended ω -3/ ω -6 ratio for human health is 0.5 to 1.0 (Simopoulos 2016), and in our study, the ω -3/ ω -6 ratio of *K. antarctica* was between 0.5 and 6.3, across all conditions.

Among all of the treatments tested, phosphorus starvation was an effective strategy to produce a quality fatty acid profile. Phosphorus-starved cells contained the highest amount of

PUFAs (90.6 mg g⁻¹ DW, 50.8% TFA) and ω -3 fatty acids (43.6 mg g⁻¹ DW, 24.5% TFA), with an ω -3/ ω -6 ratio of 0.9. The essential fatty acids LA and ALA were also more abundant in P-starved cells, compared with the other stress treatments. Although OA constituted a third (32.3%) of the TFAs in P-starved cells, valuable PUFAs can be separated from other fatty acids by fractional distillation or winterization (Mendes et al. 2007; Cuellar-Bermudez et al. 2015). Both natural and refined microalgae oils could be used as sources of food and feed and in nutraceutical and pharmacological applications (Adarme-Vega et al. 2012).

LC-PUFA production by *Koliella antarctica*

Only a subset of microalgae species have the necessary metabolic pathways to produce LC-PUFAs with chain lengths of C20 and beyond (Mühlroth et al. 2013). Therefore, strains such as *K. antarctica* that can produce EPA and ARA are potentially valuable cell factories. Our fatty acid identifications are concordant with those of Lang et al. (2011), who also identified the production of ARA and EPA in *K. antarctica*. In the present study, the highest EPA content amounted to 6.7 mg g⁻¹ DW (4.9% TFA) in control treatments. However, this was almost matched by cells under P starvation and HS conditions, each of which contained comparable total amounts of EPA at 5.4 mg g⁻¹ DW (3.1 and 5.0% of TFA, respectively). The proportion of EPA produced by *K. antarctica* was similar to *Tetraselmis chuii*, a microalga commonly used in aquafeeds, in which EPA accounted for 5.0% of TFA (Lang et al. 2011). In the bubble tube experiments, the accumulation of ARA in *K. antarctica* was induced by both N and P starvation, but it was more enhanced by N starvation than by P starvation. The highest ARA content of 9.6 mg g⁻¹ DW (3.5% of TFA) was found under 250 μ mol m⁻² s⁻¹ after prolonged nutrient starvation in the flat-plate photobioreactor, and its proportion was comparable to other candidate strains for ARA production, including *P. tricornutum* (Řezanka et al. 2014).

EPA can be synthesized via the ω -3 and ω -6 pathways in microalgae (Guschina and Harwood 2006). Here, the presence of the intermediate fatty acid ARA implicates at least a role for the ω -6 route in *K. antarctica*. The ω -6 pathway is also the dominant metabolic pathway in the EPA-rich eustigmatophyte *Nannochloropsis* (Schneider and Roessler 1994; Shene et al. 2016). However, the exact nature of LC-PUFA biosynthesis in *K. antarctica*, including the regulation of metabolic pathways, merits further investigation.

Protein content of *Koliella antarctica*

Nutritional and toxicological tests have reported that microalgae biomass is often suitable as a protein-rich feed

supplement or could replace conventional protein sources (Yaakob et al. 2014). However, under certain stress conditions, the carbon fixed by microalgae is partitioned toward carbohydrate or lipid synthesis, rather than protein synthesis (Hu et al. 2008). Our results showed that phosphorus-starved cells maintained the highest protein content of 31.4% DW, while the nitrogen-starved cells recorded the lowest protein content of 12.2%. Therefore, *K. antarctica* can accumulate fatty acids under P starvation while simultaneously maintaining the protein content. This feature could make the microalga a suitable whole-cell ingredient for animal and aqua feeds, in which both high protein and lipid contents are desired (Wells et al. 2017). However, the nutritional value of protein in *K. antarctica* needs to be evaluated by assessing its amino acid profile and conducting digestibility studies.

Cultivation of *Koliella antarctica* in intensive flat-plate photobioreactors

The cultivation of microalgae in intensive conditions, including high light, is an important step toward developing systems that can be deployed at larger scale, potentially outdoors. Light intensity is an especially important parameter for industrial microalgae production because it influences cell growth and photosynthetic efficiency and changes the biochemical composition of microalgae (He et al. 2015). Here, the maximum biomass yield on light was the highest (1.05 g mol⁻¹ photons) at 70 μ mol photons m⁻² s⁻¹, but it decreased to 0.27 g mol⁻¹ photons at 500 μ mol photons m⁻² s⁻¹. At low irradiances, higher photosynthetic efficiency can be obtained because heat dissipation by non-photochemical quenching (NPQ) or chlorophyll fluorescence is minimized (Müller et al. 2001). The maximum biomass yield on light at a PPFD of 70 μ mol photons m⁻² s⁻¹ was comparable to those obtained in other studies at warmer temperatures. For example, values of 1.25 and 1.11 g mol⁻¹ photons were obtained at low light intensities using the model alga *Chlamydomonas reinhardtii* (Takache et al. 2010; Kliphuis et al. 2012).

The attenuated growth at 500 μ mol photons m⁻² s⁻¹ in Li-Ex I could be attributed to the combined effects of nutrient and CO₂ supply, coupled with the high irradiance. Especially, the high rate of nitrogen consumption in Li-Ex I likely suppressed protein biosynthesis and impaired photosynthetic performance (Ho et al. 2012). The negative effects of high irradiance can be mitigated to an extent by supplying excess nutrients and CO₂, while allowing the cell density to increase to improve mutual shading (Chen et al. 2011). When these adjustments were made in Li-Ex II, the maximum productivity of *K. antarctica* was substantially improved to 2.37 g L⁻¹ day⁻¹, and the maximum biomass yield on light was enhanced proportionally to 0.73 g mol⁻¹ photons. To our knowledge, this is among the higher biomass productivities obtained at

temperatures ≤ 15 °C, and one of few studies that have used optimized photobioreactor platforms to cultivate polar microalgae. Although the results of this study are promising, our experiments used a maximum irradiance of $500 \mu\text{mol photons m}^{-2} \text{s}^{-1}$. Future studies might therefore extend this work by testing the effects of higher and/or variable light conditions. Especially, the combined effects of temperature and high light should be investigated, to test the suitability of *K. antarctica* for possible outdoor cultivation systems in cooler climates.

Conclusions

Koliella antarctica exhibited maximum biomass productivity of $2.37 \text{ g L}^{-1} \text{ day}^{-1}$ at 15 °C after culture optimization and tolerated a relatively broad range of salinities. The highest total fatty acid content obtained was 271.9 mg g^{-1} dry weight. Nitrogen and phosphorus starvation strongly induced TAG accumulation up to 90.3% TFA, which mostly consisted of the monounsaturated fatty acid OA. However, PUFAs were also abundant and together accounted for 30.3–45.8% of total TAG. The highest amount of EPA was $6.7 \text{ mg g}^{-1} \text{ DW}$ (4.9% TFA) in the control treatments. ARA accumulation mostly occurred in TAG and was largely induced by nitrogen starvation, reaching $9.6 \text{ mg g}^{-1} \text{ DW}$ (3.5% TFA) in the late stationary phase. Phosphorus starvation was an effective strategy to obtain high fatty acid contents, while also maintaining the protein content. Phosphorus-starved cells also contained the highest total PUFAs and omega-3 fatty acids. The high productivity of *K. antarctica* at cooler temperatures concurrent with production of high-value LC-PUFAs could make this strain a potential candidate for producing food and feed ingredients, possibly offering the opportunity for cultivation in cooler climates or during the winter in temperate regions.

Acknowledgements The authors thank the Nord University for project support, especially the Aquaculture MS program, for the staff and infrastructure provided at the university research station. The authors thank the Nordland County Government for the funding, as part of the project “Bioteknologi—en framtidens næring.” The authors are grateful to Bisa Saraswathy for providing input on earlier drafts of this manuscript. The authors also wish to thank three anonymous reviewers for their valuable feedback on the manuscript. CJH is grateful for support from a European Commission Marie Skłodowska-Curie individual fellowship (No. 749910).

Author contributions HS planned and conducted the study with guidance from CJH, KV, and RHW. HS analyzed the samples and data with assistance from CJH. HS wrote the manuscript with input from CJH, KV, and RHW.

Compliance with ethical standards

Competing interests The authors declare that they have no competing interests.

Open Access This article is distributed under the terms of the Creative Commons Attribution 4.0 International License (<http://creativecommons.org/licenses/by/4.0/>), which permits use, duplication, adaptation, distribution and reproduction in any medium or format, as long as you give appropriate credit to the original author(s) and the source, provide a link to the Creative Commons license, and indicate if changes were made.

References

- Abedi E, Sahari MA (2014) Long-chain polyunsaturated fatty acid sources and evaluation of their nutritional and functional properties. *Food Sci Nutr* 2:443–463
- Adarme-Vega TC, Lim DKY, Timmins M, Vernen F, Li Y, Schenk PM (2012) Microalgal biofactories: a promising approach towards sustainable omega-3 fatty acid production. *Microb Cell Factories* 11:96
- Andreoli C, Lokhorst GM, Mani AM, Scarabel L, Moro I, La Rocca N, Tognetto L (1998) *Koliella antarctica* sp. nov. (Klebsormidiales) a new marine green microalga from the Ross Sea (Antarctica). *Algal Stud/Arch Hydrobiol Suppl* 90:1–8
- Andreoli C, Moro I, La Rocca N, Valle LD, Masiero L, Rascio N, Vecchia FD (2000) Ecological, physiological, and biomolecular surveys on microalgae from Ross Sea (Antarctica). *Ital J Zool* 67(S1):147–156
- Artamonova EY, Svenning JB, Vasskog T, Hansen E, Eilertsen HC (2017) Analysis of phospholipids and neutral lipids in three common northern cold water diatoms: *Coscinodiscus concinnus*, *Porosira glacialis*, and *Chaetoceros socialis*, by ultra-high performance liquid chromatography-mass spectrometry. *J Appl Phycol* 29:1241–1249
- Bigogno C, Khozin-Goldberg I, Cohen Z (2002) Accumulation of arachidonic acid-rich triacylglycerols in the microalga *Parietochloris incisa* (Trebuxiophyceae, Chlorophyta). *Phytochemistry* 60:135–143
- Bischoff HW, Bold HC (1963) Phycological studies. IV. Some soil algae from enchanted rock and related algal species. University of Texas Publications 6318:1–95
- Boelen P, van Dijk R, Sinnighe Damsté JS, Rijpstra WIC, Buma AGJ (2013) On the potential application of polar and temperate marine microalgae for EPA and DHA production. *AMB Express* 3:26–26
- Borowitzka MA (2013) High-value products from microalgae—their development and commercialisation. *J Appl Phycol* 25:743–756
- Chen B, Wan C, Mehmood MA, Chang J-S, Bai F, Zhao X (2017) Manipulating environmental stresses and stress tolerance of microalgae for enhanced production of lipids and value-added products—a review. *Bioresour Technol* 244:1198–1206
- Chen C-Y, Yeh K-L, Aisyah R, Lee D-J, Chang J-S (2011) Cultivation, photobioreactor design and harvesting of microalgae for biodiesel production: a critical review. *Bioresour Technol* 102:71–81
- Chisti Y (2013) Constraints to commercialization of algal fuels. *J Biotechnol* 167:201–214
- Chrimadha T, Borowitzka MA (1994) Effect of cell density and irradiance on growth, proximate composition and eicosapentaenoic acid production of *Phaeodactylum tricorutum* grown in a tubular photobioreactor. *J Appl Phycol* 6:67–74
- Cuellar-Bermudez SP, Aguilar-Hernandez I, Cardenas-Chavez DL, Ornelas-Soto N, Romero-Ogawa MA, Parra-Saldivar R (2015) Extraction and purification of high-value metabolites from microalgae: essential lipids, astaxanthin and phycobiliproteins. *Microb Biotechnol* 8:190–209
- Ferroni L, Baldissarotto C, Zennaro V, Soldani C, Fasulo MP, Pancaldi S (2007) Acclimation to darkness in the marine chlorophyte *Koliella antarctica* cultured under low salinity: hypotheses on its origin in the polar environment. *Eur J Phycol* 42:91–104

- Glencross BD (2009) Exploring the nutritional demand for essential fatty acids by aquaculture species. *Rev Aquacult* 1:71–124
- Guieysse B, Béchet Q, Shilton A (2013) Variability and uncertainty in water demand and water footprint assessments of fresh algae cultivation based on case studies from five climatic regions. *Bioresour Technol* 128:317–323
- Guiheneuf F, Stengel DB (2013) LC-PUFA-enriched oil production by microalgae: accumulation of lipid and triacylglycerols containing n-3 LC-PUFA is triggered by nitrogen limitation and inorganic carbon availability in the marine haptophyte *Pavlova lutheri*. *Mar Drugs* 11:4246–4266
- Guschina IA, Harwood JL (2006) Lipids and lipid metabolism in eukaryotic algae. *Progr Lipid Res* 45:160–186
- He Q, Yang H, Wu L, Hu C (2015) Effect of light intensity on physiological changes, carbon allocation and neutral lipid accumulation in oleaginous microalgae. *Bioresour Technol* 191:219–228
- Ho S-H, Chen C-Y, Chang J-S (2012) Effect of light intensity and nitrogen starvation on CO₂ fixation and lipid/carbohydrate production of an indigenous microalga *Scenedesmus obliquus* CNW-N. *Bioresour Technol* 113:244–252
- Hu Q, Sommerfeld M, Jarvis E, Ghirardi M, Posewitz M, Seibert M, Darzins A (2008) Microalgal triacylglycerols as feedstocks for biofuel production: perspectives and advances. *Plant J* 54:621–639
- Hulatt CJ, Berecz O, Egeland ES, Wijffels RH, Kiron V (2017) Polar snow algae as a valuable source of lipids? *Bioresour Technol* 235:338–347
- Ishika T, Moheimani NR, Bahri PA (2017) Sustainable saline microalgae co-cultivation for biofuel production: a critical review. *Renew Sust Energy Rev* 78:356–368
- Khozin-Goldberg I, Iskandarov U, Cohen Z (2011) LC-PUFA from photosynthetic microalgae: occurrence, biosynthesis, and prospects in biotechnology. *Appl Microbiol Biotechnol* 91:905–915
- Kliphuis AMJ, Klok AJ, Martens DE, Lamers PP, Janssen M, Wijffels RH (2012) Metabolic modeling of *Chlamydomonas reinhardtii*: energy requirements for photoautotrophic growth and maintenance. *J Appl Phycol* 24:253–266
- Klok AJ, Lamers PP, Martens DE, Draaisma RB, Wijffels RH (2014) Edible oils from microalgae: insights in TAG accumulation. *Trends Biotechnol* 32:521–528
- Kvíděrová J, Shukla SP, Pushparaj B, Elster J (2017) Perspectives of low-temperature biomass production of polar microalgae and biotechnology expansion into high latitudes. In: Margesin R (ed) *Psychrophiles: from biodiversity to biotechnology*. Springer, Cham, pp 585–600
- La Rocca N, Sciuto K, Meneghesso A, Moro I, Rascio N, Morosinotto T (2015) Photosynthesis in extreme environments: responses to different light regimes in the Antarctic alga *Koliella antarctica*. *Physiol Plant* 153:654–667
- Lang I, Hodac L, Friedl T, Feussner I (2011) Fatty acid profiles and their distribution patterns in microalgae: a comprehensive analysis of more than 2000 strains from the SAG culture collection. *BMC Plant Biol* 11:124
- Liu J, Sommerfeld M, Hu Q (2013) Screening and characterization of *Isochrysis* strains and optimization of culture conditions for docosahexaenoic acid production. *Appl Microbiol Biotechnol* 97:4785–4798
- Lourenço SO, Barbarino E, Lavín PL, Lanfer Marquez UM, Aïdar E (2004) Distribution of intracellular nitrogen in marine microalgae: calculation of new nitrogen-to-protein conversion factors. *Eur J Phycol* 39:17–32
- Marchetti J, da Costa F, Bougaran G, Quéré C, Soudant P, Robert R (2018) The combined effects of blue light and dilution rate on lipid class and fatty acid composition of *Tisochrysis lutea*. *J Appl Phycol* 30:1483–1494
- Markou G, Nerantzis E (2013) Microalgae for high-value compounds and biofuels production: a review with focus on cultivation under stress conditions. *Biotechnol Adv* 31:1532–1542
- Martínez-Roldán AJ, Perales-Vela HV, Cañizares-Villanueva RO, Torzillo G (2014) Physiological response of *Nannochloropsis* sp. to saline stress in laboratory batch cultures. *J Appl Phycol* 26:115–121
- Martins DA, Custódio L, Barreira L, Pereira H, Ben-Hamadou R, Varela J, Abu-Salah KM (2013) Alternative sources of n-3 long-chain polyunsaturated fatty acids in marine microalgae. *Mar Drugs* 11:2259–2281
- Mendes A, da Silva TL, Reis A (2007) DHA concentration and purification from the marine heterotrophic microalga *Crypthecodinium cohnii* CCMP 316 by winterization and urea complexation. *Food Technol Biotechnol* 45:38
- Morgan-Kiss RM, Priscu JC, Pockock T, Gudynaite-Savitch L, Huner NPA (2006) Adaptation and acclimation of photosynthetic microorganisms to permanently cold environments. *Microbiol Mol Biol Rev* 70:222–252
- Mühlroth A, Li K, Røkke G, Winge P, Olsen Y, Hohmann-Marriott M, Vadstein O, Bones A (2013) Pathways of lipid metabolism in marine algae, co-expression network, bottlenecks and candidate genes for enhanced production of EPA and DHA in species of Chromista. *Mar Drugs* 11(11):4662–4697
- Müller P, Li X-P, Niyogi KK (2001) Non-photochemical quenching. A response to excess light energy. *Plant Physiol* 125:1558–1566
- Pal D, Khozin-Goldberg I, Cohen Z, Boussiba S (2011) The effect of light, salinity, and nitrogen availability on lipid production by *Nannochloropsis* sp. *Appl Microbiol Biotechnol* 90:1429–1441
- Procházková G, Brányiková I, Zachleder V, Brányik T (2014) Effect of nutrient supply status on biomass composition of eukaryotic green microalgae. *J Appl Phycol* 26:1359–1377
- Procházková L, Remias D, Holzinger A, Řezanka T, Nedbalová L (2018) Ecophysiological and morphological comparison of two populations of *Chlainomonas* sp. (Chlorophyta) causing red snow on ice-covered lakes in the High Tatras and Austrian Alps. *Eur J Phycol* 53:230–243
- Řezanka T, Lukavský J, Nedbalová L, Sigler K (2014) Production of structured triacylglycerols from microalgae. *Phytochemistry* 104:95–104
- Ringuet S, Sassano L, Johnson ZI (2011) A suite of microplate reader-based colorimetric methods to quantify ammonium, nitrate, orthophosphate and silicate concentrations for aquatic nutrient monitoring. *J Environ Monit* 13:370–376
- Salama el S, Kim HC, Abou-Shanab RA, Ji MK, Oh YK, Kim SH, Jeon BH (2013) Biomass, lipid content, and fatty acid composition of freshwater *Chlamydomonas mexicana* and *Scenedesmus obliquus* grown under salt stress. *Bioprocess Biosyst Eng* 36:827–833
- Schneider JC, Roessler P (1994) Radiolabeling studies of lipids and fatty acids in *Nannochloropsis* (Eustigmatophyceae), an oleaginous marine alga. *J Phycol* 30:594–598
- Sharma KK, Schuhmann H, Schenk PM (2012) High lipid induction in microalgae for biodiesel production. *Energies* 5:1532–1553
- Shene C, Chisti Y, Vergara D, Burgos-Díaz C, Rubilar M, Bustamante M (2016) Production of eicosapentaenoic acid by *Nannochloropsis oculata*: effects of carbon dioxide and glycerol. *J Biotech* 239:47–56
- Simopoulos PA (2016) An increase in the omega-6/omega-3 fatty acid ratio increases the risk for obesity. *Nutrients* 8:128
- Spijkerman E, Wacker A, Weithoff G, Leya T (2012) Elemental and fatty acid composition of snow algae in Arctic habitats. *Front Microbiol* 3:380
- Takache H, Christophe G, Comet JF, Pruvost J (2010) Experimental and theoretical assessment of maximum productivities for the

- microalgae *Chlamydomonas reinhardtii* in two different geometries of photobioreactors. *Biotechnol Prog* 26:431–440
- Team RC (2018) R: a language and environment for statistical computing
- Teoh M-L, Chu W-L, Marchant H, Phang S-M (2004) Influence of culture temperature on the growth, biochemical composition and fatty acid profiles of six Antarctic microalgae. *J Appl Phycol* 16:421–430
- Tonon T, Harvey D, Larson TR, Graham IA (2002) Long chain polyunsaturated fatty acid production and partitioning to triacylglycerols in four microalgae. *Phytochemistry* 61:15–24
- von Alvensleben N, Magnusson M, Heimann K (2016) Salinity tolerance of four freshwater microalgal species and the effects of salinity and nutrient limitation on biochemical profiles. *J Appl Phycol* 28:861–876
- Vona V, Di Martino RV, Lobosco O, Carfagna S, Esposito S, Rigano C (2004) Temperature responses of growth, photosynthesis, respiration and NADH: nitrate reductase in cryophilic and mesophilic algae. *New Phytol* 163:325–331
- Wells ML, Potin P, Craigie JS, Raven JA, Merchant SS, Helliwell KE, Smith AG, Camire ME, Brawley SH (2017) Algae as nutritional and functional food sources: revisiting our understanding. *J Appl Phycol* 29:949–982
- Wijffels RH, Barbosa MJ (2010) An outlook on microalgal biofuels. *Science* 329:796–799
- Yaakob Z, Ali E, Zainal A, Mohamad M, Takriff MS (2014) An overview: biomolecules from microalgae for animal feed and aquaculture. *J Biol Res (Thessaloniki)* 21:6